Developmental Biology **247,** 165–181 (2002)
doi:10.1006/dbio.2002.0673

The Planar Cell Polarity Gene *Strabismus* Regulates Convergence and Extension and Neural Fold Closure in *Xenopus*

Toshiyasu Goto[1] **and Ray Keller**

Department of Biology, Gilmer Hall, University of Virginia, Charlottesville, Virginia 22903

We cloned *Xenopus Strabismus* (*Xstbm*), a homologue of the *Drosophila* planar cell or tissue polarity gene. *Xstbm* encodes four transmembrane domains in its N-terminal half and a PDZ-binding motif in its C-terminal region, a structure similar to *Drosophila* and mouse homologues. *Xstbm* is expressed strongly in the deep cells of the anterior neural plate and at lower levels in the posterior notochordal and neural regions during convergent extension. Overexpression of *Xstbm* inhibits convergent extension of mesodermal and neural tissues, as well as neural tube closure, without direct effects on tissue differentiation. Expression of *Xstbm(ΔPDZ-B)*, which lacks the PDZ-binding region of *Xstbm*, inhibits convergent extension when expressed alone but rescues the effect of overexpressing *Xstbm*, suggesting that *Xstbm(ΔPDZ-B)* acts as a dominant negative and that both increase and decrease of Xstbm function from an optimum retards convergence and extension. Recordings show that cells expressing *Xstbm* or *Xstbm(ΔPDZ-B)* fail to acquire the polarized protrusive activity underlying normal cell intercalation during convergent extension of both mesodermal and neural and that this effect is population size-dependent. These results further characterize the role of *Xstbm* in regulating the cell polarity driving convergence and extension in *Xenopus*.

Key Words: **gastrulation; neurulation; convergence; extension; polarity; *strabismus*; *Van Gogh*; motility; PDZ-B; *Xenopus*.**

INTRODUCTION

The convergence and extension of the axial and paraxial mesoderm and neural tissues of *Xenopus* play a large role in gastrulation, body axis formation, and subsequent neural and mesodermal tissue morphogenesis (Keller *et al.*, 2000). Convergent extension of these tissues occurs by two types of active and force-producing cell intercalations. The first of these is radial intercalation in the early gastrula, a movement in which several layers of deep cells rearrange to form fewer layers of greater length (thinning and extension) (Wilson *et al.*, 1989; Wilson and Keller, 1991). At the midgastrula stage, the deep prospective dorsal posterior mesodermal cells and the deep prospective posterior neural cells begin intercalation along the mediolateral axis (mediolateral intercalation) to form a narrower, longer array (convergence and extension) (see Keller and Tibbetts, 1989).

Mediolateral cell intercalation involves polarized cell behaviors. Deep prospective notochordal and somitic mesodermal cells become bipolar, extending protrusions both medially and laterally, exerting traction on their neighbors, and pulling themselves together along this axis, undergoing mediolateral intercalation, and thereby forming a longer, narrower array (Shih and Keller, 1992a,b; Keller *et al.*, 2000). In contrast, the posterior deep neural cells undergo mediolateral intercalation by becoming monopolar with their protrusive activity directed toward the midline tissues of notoplate and notochord (Elul and Keller, 2000; M. Ezin, unpublished observations). It is not understood how these cells become polarized in these differing fashions.

However, recent work shows that components of the planar cell or tissue polarity pathway that control epithelial cell polarity of sensory bristles and the eye of *Drosophila* (Adler and Taylor, 2001; Adler and Lee, 2001; Strutt and Strutt, 1999; Mlodzik, 1999; Shulman *et al.*, 1998; McEwen and Peifer, 2000) are also involved in convergence and extension of vertebrates. The seven-pass transmembrane receptor, Frizzled, which functions in the canonical Wnt pathway, also controls tissue polarity in the wing (Vinson and Adler, 1987; Vinson *et al.*, 1989; Wong and Adler, 1993; Park *et al.*, 1994; Adler *et al.*, 1997; Strutt, 2001) and in eye

[1] To whom correspondence should be addressed. Fax: (434) 982-5626. E-mail: tg4j@virginia.edu.

0012-1606/02 $35.00

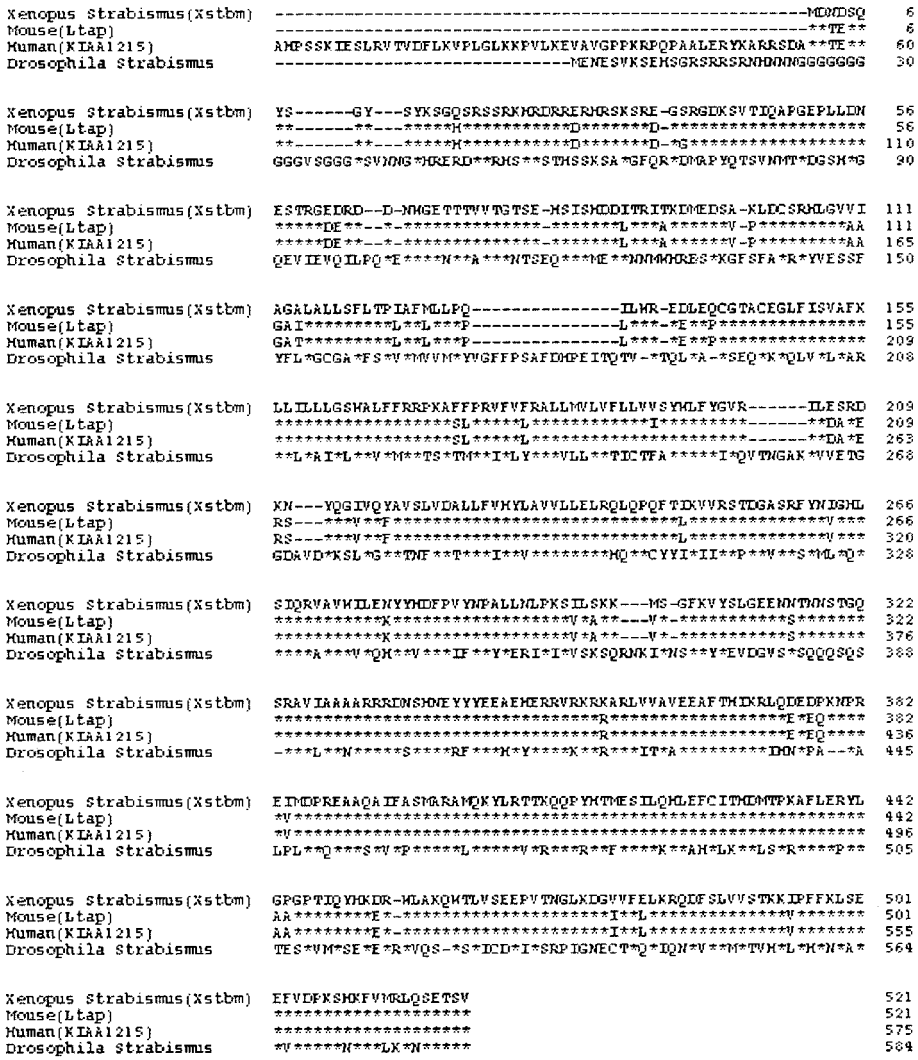

FIG. 1. Alignment of the Xstbm, mouse Ltap, human KIAA1215 and *Drosophila* Strabismus amino acid sequences. The conserved amino acids are represented by asterisks (*). The PDZ-binding domains are shaded gray.

of *Drosophila* (Zheng *et al.*, 1995; Strutt *et al.*, 1997), also functions in convergence and extension (Deardorff *et al.*, 1998; Djiane *et al.*, 2000; Medina *et al.*, 2000) as well as in tissue separation (Winklbauer *et al.*, 2001) in frogs. Frizzled signaling requires Dishevelled (Dsh), which functions in the canonical Wingless/Wnt/β catenin signaling pathway as well as the noncanonical, planar cell polarity pathway of *Drosophila* (Klingensmith *et al.*, 1994; Theisen *et al.*, 1994; Krasnow *et al.*, 1995; Axelrod *et al.*, 1998; Boutros and Mlodzik, 1999). Forms of Dsh that regulate cell polarity but do not function in the canonical Wnt pathway in *Drosophila* (Axelrod *et al.*, 1998; Boutros *et al.*, 1998; Rothbacher *et al.*, 2000) also affect convergence and extension in frogs without apparent effect on tissue determination (Sokol, 1996, 2000; Wallingford *et al.*, 2000; Wallingford and Harland, 2001). Although the Frizzled ligand functioning in the tissue polarity pathway of *Drosophila* is unknown, a dominant negative form of Wnt 11 inhibits convergence and extension in frogs (Tada and Smith, 2000). A loss-of-function of the zebrafish gene, Silberblick, which encodes Wnt 11, inhibits extension (Heisenberg *et al.*, 2000). In both the frog and fish studies, these defects are rescued by forms of Dsh that are inactive in the canonical Wnt/β catenin pathway. Wnt 5a also appears to affect convergence and extension in frogs (Moon *et al.*, 1993). There is also evidence that signaling through the Ca/Wnt pathway (Kuhl *et al.*, 2000) is necessary for expression of Xnr3, an essential component for convergence and extension (Kuhl *et al.*, 2001). Recent studies show that Wnt/Frizzled signaling activates the cytoskeletal regulator, Rho, and requires direct interaction of Dishevelled with Daam1 (dishevelled associated activator of morphogenesis), a formin-homology

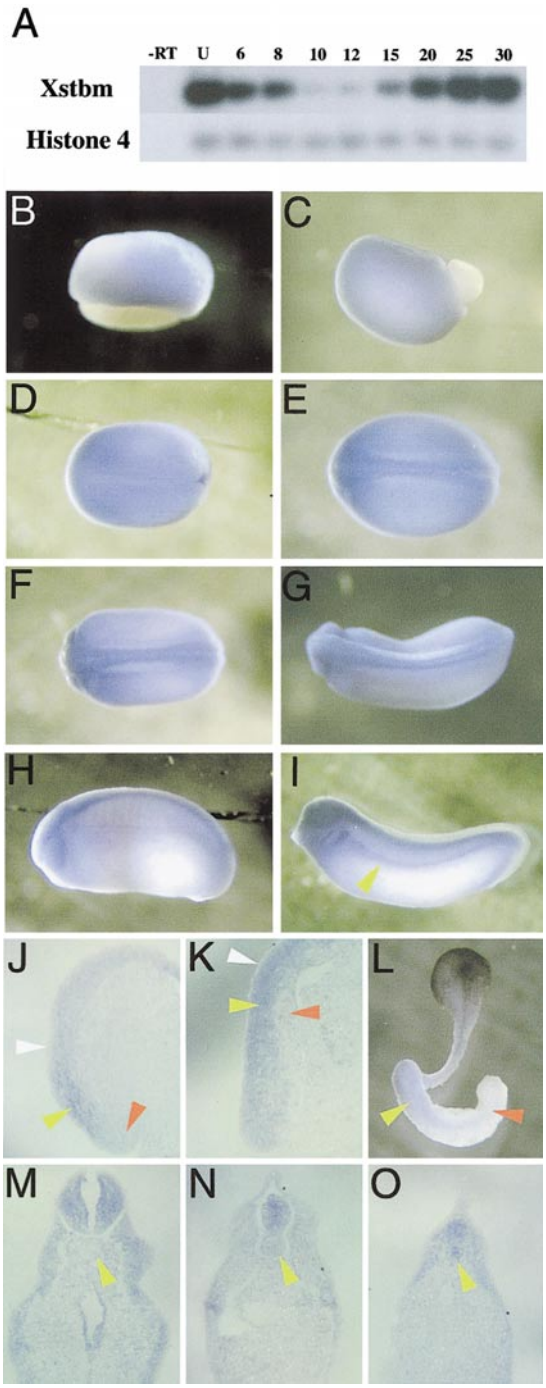

FIG. 2. Temporal and spatial expression of *Xstbm*. (A) Quantitative RT-PCR was performed by using 1 μg of total RNA extracted from *Xenopus* embryos at different stages. "U" indicates the unfertilized eggs, and numbers indicate the developmental stages according to Nieuwkoop and Faber (1967). Maternal transcripts decreased gradually until the gastrula stage (stage 10), and zygotic expression increased thereafter in the gastrula (stage 12) and neurula (stage 15–20). (B–O) Localization of *Xstbm* transcripts by whole-mount *in situ* hybridization. At the gastrula stage, *Xstbm* is expressed in the dorsal region (B, dorsal view, stage 10; C, lateral view, stage 12). *Xstbm* is expressed in the neural plate of the early neurula (D, stage 14) and late neurula (E, stage 17), and in the neural tube thereafter in the tailbud stages (F, stage 20; G, stage 25, dorsal view; H, stage 25, lateral view; I, stage 30, lateral view). At tailbud stage, *Xstbm* is also expressed in prenephritic region (I, yellow pointer). Sections of the gastrula (B, C) show low expression at the dorsal lip (red pointer) and higher expression in the posterior mesodermal–neural region (yellow pointer) above the blastoporal lip (J, stage 10). The late gastrula shows high expression in the prospective forebrain (K, stage 12, yellow pointer) and low expression in the anterior mesodermal region (K, red pointer). The superficial epithelial layer of the involuting mesodermal region showed little or no expression at stage 10 (J, white pointer) and stage 12 (K, white pointer). The posterior mesodermal regions of a dorsal sandwich explant showed expression at the late neurula stage (L, yellow pointer), but expression declined anteriorly (L, red pointer). Transverse sections of a tailbud stage embryo in (I) showed the expression of *Xstbm* increased progressively from the anterior (M, yellow pointer) to the middle (N, yellow pointer) and posterior notochord (O, yellow pointer).

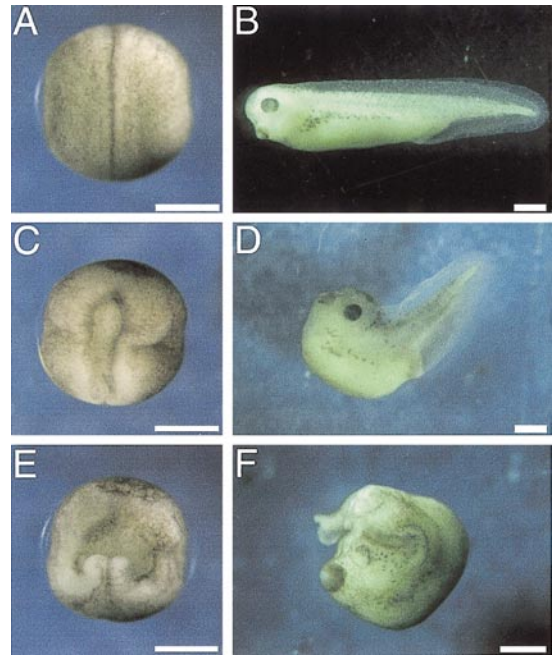

FIG. 3. Overexpression of *Xstbm* interfered with posterior neural fold fusion and closure of the neural folds to form the neural tube. (A, C, E) Neurula-stage embryos (stage 20). (B, D, F) Tailbud-stage embryos (stage 30). (A, B) Normal embryos. (C, D) Under moderate doses of *Xstbm*, neural fold fusion and posterior neural tube closure were impaired, and the dorsal axial and paraxial tissues and the neural plate did not converge and extend well. (E, F) Under larger doses, neural fold fusion did not occur and the dorsal axial tissues were very short in the anterior–posterior axis. Bars, 0.5 mm.

protein that binds to both dishevelled and Rho, in both human cell lines and in *Xenopus* (Habas *et al.*, 2001). They show that Daam1 is required in the Wnt/Rho signaling pathway for gastrulation in *Xenopus*. A glypican Knipek

(Topczewski *et al.*, 2001) has been implicated in potentiating Wnt signaling during convergence and extension in the zebrafish, and there is evidence that integrin-mediated interactions of cells with fibronectin function in setting up polarized cell behaviors (Marsden and DeSimone, 2001).

In *Drosophila*, the gene *Van Gogh/strabismus* regulates tissue polarity in the legs, wing (Taylor *et al.*, 1998; Adler *et al.*, 2000), and eye (Wolff and Rubin, 1998). It appears to act antagonistically to Frizzled and shows the cell-nonautonomous property of altering cell polarity of normal cells outside clones of cells null for this gene, having the opposite effect on cell polarity from comparable Frizzled clones in this regard (Taylor *et al.*, 1998). Overexpression and morpholino-mediated repression suggest that the planar cell polarity gene Strabismus (stbm)/Van Gogh (Vang) affects cell fate and convergence and extension movements in zebrafish and *Xenopus* (Park and Moon, 2002; Darken *et al.*, 2002). The mechanisms by which Strabismus functions in convergence and extension of vertebrates remains uncharacterized.

As these facts suggest that the cell polarity involved in convergence and extension, described above, shares underlying mechanisms with the *Drosophila* planar cell or tissue polarity pathway, we have cloned and characterized the expression and function of several planar cell polarity pathway components in *Xenopus*, including *Prickle* (Wallingford *et al.*, 2002) and *Van Gogh/strabismus*. Here, we characterize the function of *Xenopus strabismus* in terms of changes in cell motility and polarized protrusive activity with direct visualization of cell motility during convergence and extension.

MATERIALS AND METHODS

Eggs and Embryos

Eggs were obtained by injecting *Xenopus laevis* females with human chorionic gonadotropin and fertilizing them *in vitro* by standard methods. Embryos were dejellied by a standard method and cultured in 30% modified Barth's saline (MBS). Developmental stages were determined according to Nieuwkoop and Faber (1967).

Cloning of Xstbm and Constructing Xstbm(ΔPDZ-B) and Xstbm(ΔTM)

Total RNA was isolated by the acid guanidinium thiocyanate-phenol-chloroform method (Chomczynski and Sacchi, 1987) from stage 10 embryos. A cDNA fragment of *Xstbm* was obtained by RT-PCR using the degenerate forward 5′-ATGACHCCHAAGGCTTTYCTBGAR-3′ and reverse 5′-ACAAAYTTRTGAGAYTTWGGGTCN-3′ primers. A full-length *Xstbm* cDNA (Accession No. AF387816) (1–521) was obtained by screening a stage 10 cDNA library, which we made using a ZAP-expression cDNA synthesis kit (Stratagene), and then it was subcloned into a pCS2+ vector. A *Xstbm* lacking the carboxy end including the putative PDZ-binding region (ESTV), *Xstbm(ΔPDZ-B)* (1–499), was made by PCR using the forward 5′-gagaggatccCTCCGAAAACATGGACAATG-3′ and reverse 5′-gcgcgaattcCTACAGCTTAAAGAAGGGGA-3′primers, and then subcloned into a pCS2+ vector after digestion with *Bam*HI and *Eco*RI. A *Xstbm* lacking the transmembrane regions *Xstbm(ΔTM)* (229–521, after an additional first methionine) was made by PCR, using the forward 5′-tataggatccGCCGCCATGGTCCACTATTT-3′ and reverse 5′-gcgcgaattcTCAAACCGAGGTCTCTGATT-3′ primers, and then subcloned into a pCS2+ vector after digestion with *Bam*HI and *Eco*RI.

RT-PCR

For RT-PCR assay of developmental expression of *Xstbm*, the forward 5′-ACATTAGTCAGCGAGGAACC-3′ and reverse 5′-AGACCTAAAAGTCCCCACTG-3′ primers were used. As an internal loading control, the primers for the ubiquitously expressed *Histone4* were included in all PCRs. The forward 5′-CGGGATAACATTCAGGGTATCACT-3′ and reverse 5′-ATCCATGGCGGTAACTGTCTTCCT-3′ primers for *Histone4* were used. Aliquots containing one-tenth of the PCR products were loaded on 2% agarose gels, electrophoresed, and transferred to nylon membrane. The membranes were hybridized to the isotope-labeled fragment of *Xstbm* and autoradiographed.

Whole-Mount in Situ Hybridization and Sectioning

Whole-mount RNA *in situ* hybridization was done by using digoxigenin-labeled RNA probe and alkaline phosphatase substrate (NBT) (Boehringer Mannheim) according to Harland (1991). After *in situ* hybridization, the stained embryos were photographed whole, with or without clearing, or embedded in Paraplast and sectioned at 10 μm, and processed for light microscopy.

Microinjection and Making Explants

Messenger RNAs encoding *Xstbm* (5–200 pg), *Xstbm(ΔPDZ-B)* (*25–1000 pg*), *Xstbm(ΔTM)* (200–1000 pg), and *GFP* (5–200 pg) or 800 pg of Alexa594, were microinjected into the prospective dorsal marginal zone of the two dorsal blastomeres of the four-cell embryo in 3% Ficoll in 30% MBS. To obtain high resolution imaging of protrusive activity, a scattering of red-labeled cells on a green (GFP) background was made by injecting 10 pg of Alexa594 (Molecular Probes) into several blastomeres of the prospective dorsal marginal zone region at stage 7 (see Elul and Keller, 2000). Dorsal sandwich explants were made from stage 10 embryos according to previously described methods (Keller, 1991). For dorsal open-faced explants, the dorsal sectors of embryos previously injected with *Xstbm*, *Xstbm(ΔPDZ-B)*, or *Xstbm(ΔTM)* mRNA, and *GFP* mRNA (green label) or Alexa594 (red label) were dissected at stage 10, and endodermal and postinvolution mesodermal cells were shaved of their inner surfaces, using an eyebrow hair knife and hair loop. Clumps of about 10 cells (for small populations) or hundreds of cells (for large populations) were removed from the GFP-labeled prospective notochord region of these explants and gently wedged into specific sites in host explants. The deep surfaces of the explants were placed on fibronectin-coated cover glasses, covered with a second cover glass, and cultured in modified Danilchik's (see Sater *et al.*, 1994). Fibronectin coating was done according to previously described methods (Davidson *et al.*, 2002). The deep surfaces of these explants were observed and recorded, using the imaging methods described below. In these explants cultured on fibronectin, the notochord and neural tissue extend laterally from the midline of the explant (see Davidson *et al.*, 2002).

For neural explants, dorsal open-faced explants were made at stage 10, and clumps of cells were removed from the GFP-labeled prospective neural region without epithelium (for small popula-

tions) or with epithelium (for large populations). A corresponding small or large site was excavated in the prospective neural region of the host embryos and the GFP-labeled populations were inserted. After healing, deep-neural-overmesoderm explants were made, without the overlying neural epithelium, at stage 12, and cultured and imaged as described previously (Elul and Keller, 2000). In making grafts from *Xstbm* + *GFP*-injected regions, the grafted cells or cell populations were excised from the central part of the GFP-labeled region as much as possible to assure inclusion of Xstbm-expressing cells. The explants were cultured in modified Danilchik's solution.

The open-faced explants on fibronectin, made according to Davidson *et al.* (2002), offer a large advantage in that they are much easier to make, and they offer a more stable preparation for imaging cell intercalation than the original open-faced explant (Shih and Keller, 1992a,b), but the axes of convergence and extension are somewhat different. In both explants, when oriented with the vegetal end at the bottom and animal end at the top of the image frame, the forming notochordal/somitic boundaries describe arcs, originating at the bottom of the field near the midline and arcing up toward the sides near the top of the image. In the original explant, convergence occurs in arcs transverse to these boundaries, and the explant extends off the bottom of the frame as the posterior notochordal and somitic mesoderm converge toward the midline. In the Davidson explant on fibronectin, the convergence is the same but the extension occurs posteriorly, parallel to the original notochordal-somitic boundary (Davidson *et al.,* 2002), which means that the notochord tends to push posteriorly off the upper lateral edge of the frame. Therefore, the anterior–posterior axis along which extension occurs can be nearly vertical far anteriorly and at the onset of the movements, and horizontal posteriorly and later in the course of the movements. The local process of convergence and extension is the same but the global mechanics of which way the explant distorts are somewhat different, probably due to the mechanics of adhesion and drag on the fibronectin. We indicate the anterior–posterior axes in the figures with dashed lines or describe them in the figure legends.

Low-Light Fluorescence Imaging

Low light, fluorescence imaging and time-lapse recording of cell behavior were done with a digital camera (Hamamatsu 4742, "Orca"), an inverted Olympus IX70 compound microscope, and a Metamorph imaging system (Universal Imaging Corp.).

RESULTS

Characterization of Xstbm

We obtained a cDNA fragment of *Xstbm* from stage 10 embryos by RT-PCR using degenerate primers (see Materials and Methods) and isolated a full-length cDNA (Genbank Accession No. AF387816) by screening a gastrula-stage cDNA library, using this fragment as a probe. The predicted Xstbm protein contains four putative transmembrane regions in the N-terminal half and a PDZ-binding motif at its C terminus (Fig. 1), similar to the structure described for other species (Wolff and Rubin, 1998; Nagase *et al.,* 1999; Kibar *et al.,* 2001). Xstbm has high identities of 90.2% with mouse Ltap, 90.2% with human KIAA1215, and lower identities of 43.6% with *Drosophila strabismus* (Fig. 1). The Xstbm described here differs only by 6 amino acids from the sequence of a Xstbm described by Park and Moon (2002) and Darken *et al.* (2002).

Maternal transcripts of *Xstbm* are present at high levels in the unfertilized egg and early embryo but decline gradually by the early gastrula stage (stage 10) (Fig. 2A). Zygotic transcripts increase by the late gastrula stage (stage 12), and expression is strong from the midneurula stage (stage 15) onward (Fig. 2A). Whole-mount RNA *in situ* hybridization shows that *Xstbm* is expressed broadly in the dorsal region of the gastrula stage (Figs. 2B and 2C). It is expressed strongly in the deep neural region of the early gastrula (Fig. 2J, yellow pointer) and at a lower level in the deep neural and the deep posterior dorsal mesoderm through the late gastrula (Fig. 2J, red pointer). In the late gastrula, it is expressed most strongly in the anterior neural region (Fig. 2K, yellow pointer) and to a lesser extent in the deep neural and deep posterior dorsal mesoderm through the late gastrula (Fig. 2K, red pointer). It was not expressed on the superficial epithelial layer (Figs. 2J and 2K, white pointer) nor in the anterior, leading edge mesendoderm of the involuting marginal zone (IMZ) (Fig. 2K). *Xstbm* is expressed throughout the neural tube during late neurulation and the tailbud stages (Figs. 2D–2I). Weak expression occurs in the prenephritic region at the late tailbud stage (Fig. 2I, yellow pointer). *Xstbm* is also expressed in both mesoderm and neural regions of the dorsal sandwich ("Keller") explants but declines in the anterior notochord (Fig. 2L, red pointer) relative to the posterior notochord at the tailbud stage (Fig. 2L, yellow pointer). Cross-sections of tailbud-stage embryos also reveal this decline in expression in anterior notochord (Figs. 2M and 2N, yellow pointer), while it remains strong in the posterior notochord (Fig. 2O, yellow pointer) and in the neural tube (Figs. 2M–2O).

Xstbm Inhibits Neural Fold Closure

Synthetic mRNA encoding full-length *Xstbm* was injected into the regions of the two dorsal blastomeres of the four-cell embryo fated to form the dorsal mesodermal and neural tissues. The injected embryos developed normally until the formation of the blastopore (formation of bottle cells) was complete on the ventral side at stage 10.5, at which point closure of the blastopore was delayed or stopped. During neurulation, the neural folds failed to close, or closed poorly, depending on the dose of *Xstbm* mRNA (Figs. 3C and 3E), and the injected embryos had very short anterior–posterior axes (Figs. 3C–3F), compared with controls (Figs. 3A and 3B). Two hundred picograms of *Xstbm* mRNA per each of the two dorsal blastomeres of the four-cell embryo produced a severe phenotypes in which neural fold closure was completely blocked (Figs. 3E and 3F), with reduced amounts producing less severe closure defects (Figs. 3C and 3D). Overexpression of *Xstbm* shows a clear dose-dependent effect (Fig. 4). Comparable injections into the ventral side of the gastrula had no obvious effect (data not shown).

At levels of overexpression strongly affecting conver-

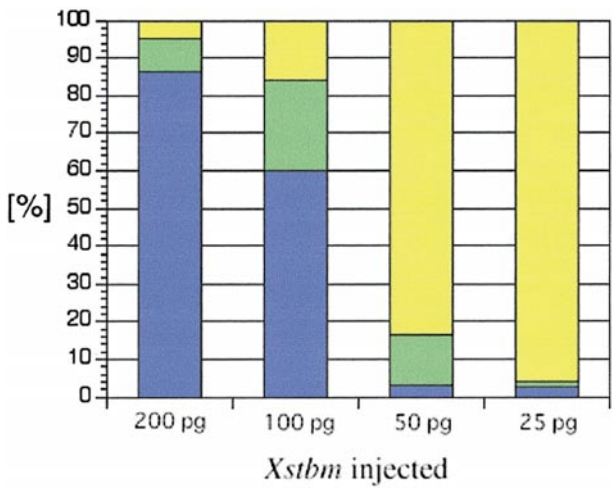

FIG. 4. Effects on phenotype by increasing doses of *Xstbm* expression. Blue bars represent ratio of embryos which were severely blocked neural fold closure as shown in Figs. 3E and 3F. Green bars represent ratio of the embryos which were impaired neural fold closure as shown in Figs. 3C and 3D. Yellow bars represent normal embryos. The proportion of severely affected embryos increased with the dose.

gence and extension, *Xstbm* does not appear to affect neural differentiation in *Xenopus*. *In situ* hybridization shows that the neural crest marker *Xslug* (Figs. 5A and 5B) and the pan-neural marker *nrp-1* (Figs. 5C and 5D) are expressed as strongly as in normal embryos but in short, wide arrays, as would be expected with reduced convergent extension and failure of neural fold apposition and fusion (Figs. 5A–5D). Expression of neural specific *n-β tubulin*, marking prospec-

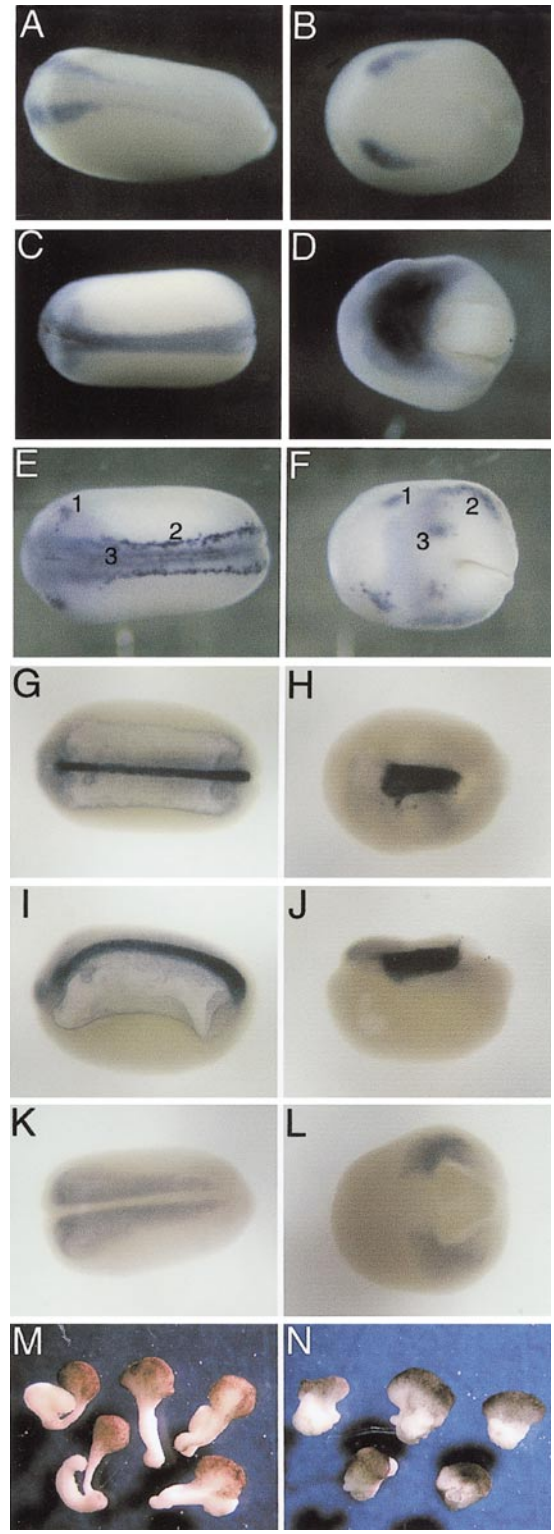

FIG. 5. Whole-mount RNA *in situ* hybridization shows expression of neural and mesodermal marker genes in *Xstbm* (200 pg)-injected embryos at stage 20 (A–L). The left column shows controls and the right column shows the corresponding *Xstbm*-injected embryos. The neural crest marker *Xslug* shows the cranial neural crest of *Xstbm*-injected embryos farther from the midline and closer to the blastopore (B), compared with the normal embryo (A). The pan-neural marker, *nrp-1*, shows a very wide, short, and unclosed neural plate typical of the *Xstbm*-injected embryos (D) compared with the elongated, converged, and fusing neural tube of normal embryo (C). The marker of prospective neurons, *n-β tubulin*, shows prospective neurons in a short array far from the midline and wrapping around the blastopore of *Xstbm* injected embryo (F), compared with the elongate, medial array in the normal embryo (E). Numbers indicate corresponding components of the expression pattern in (E) and (F). The pattern of expression of the prospective notochord marker, *chordin*, is short, wide, and thick in *Xstbm*-injected embryos (H, dorsal; J, lateral), whereas it is elongated and narrow in normal embryos (G, dorsal; I, lateral). The prospective somitic mesoderm marker, *MyoD*, is expressed around both sides of the unclosed blastopore in the *Xstbm*-injected embryo (L), whereas it is expressed in elongate arrays on both sides of the notochord in normal embryos (K). Dorsal explants of normal (control) embryos showed convergence and extension of both mesoderm and neural regions (M), whereas neither region showed convergence and extension in *Xstbm*-injected embryos (N).

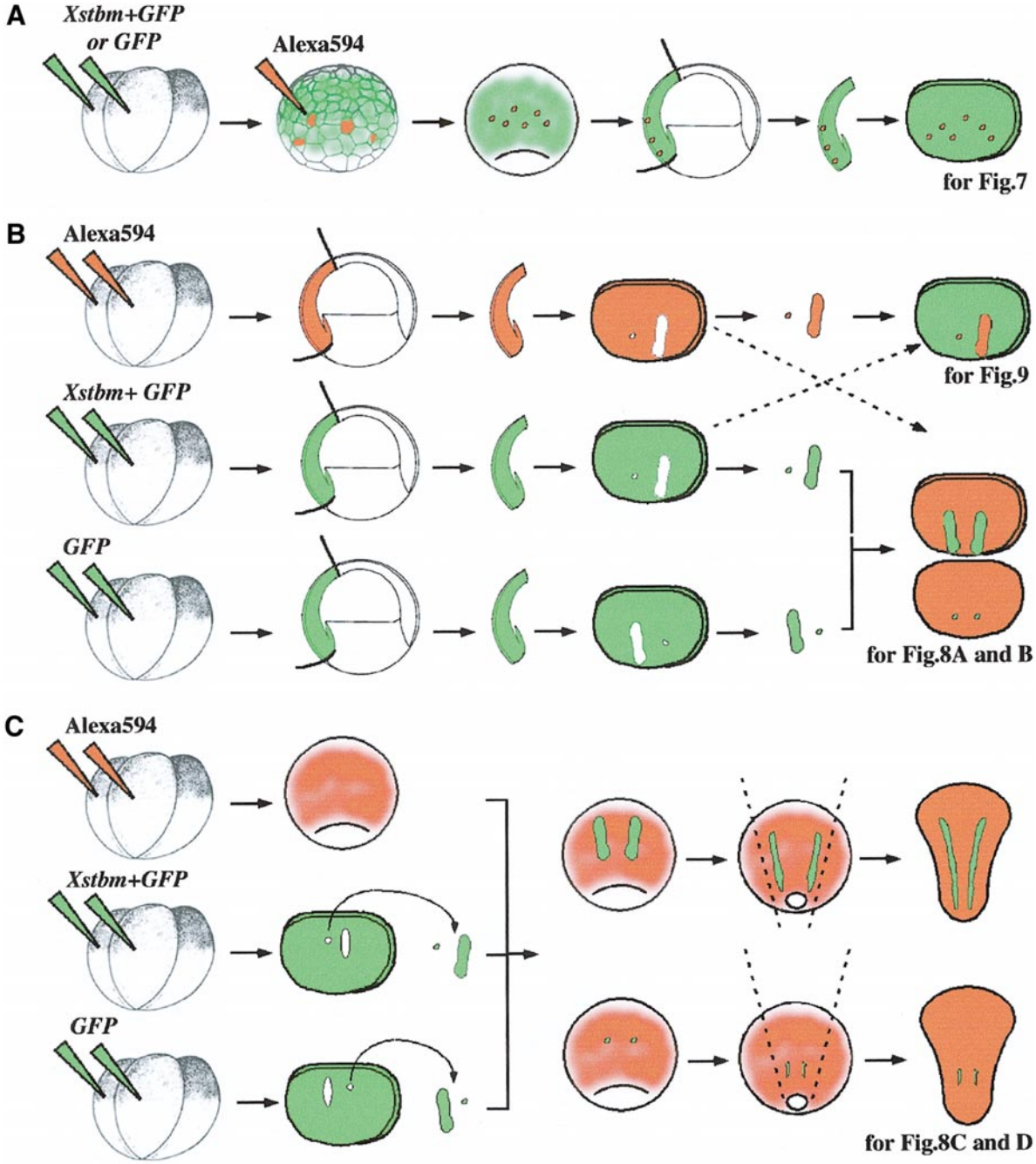

FIG. 6. Procedures for making open-faced explants. (A) Scattered double-labeled open-faced explants allow observation of cell behavior. *Xstbm* + *GFP* (200 + 200 pg) or *GFP* (200 pg) mRNA (green) was injected into two dorsal blastomeres of the four-cell-stage embryo (far left). Then, Alexa594 (10 pg; red) was injected into several dorsal blastomeres of the same embryos at stage 7 (second from left). Dorsal open-faced explants were then dissected from the injected embryos at stage 10, and any involuted endodermal and mesodermal cells were shaved off their inner surfaces before culturing for time-lapse imaging (Fig. 7). (B) Grafts between normal and *Xstbm*-injected open-faced explants were done to analyze the behavior of large and small populations of *Xstbm*-injected cells. *Xstbm* + *GFP* (200 + 200 pg), *GFP* (200 pg) mRNA (green), or Alexa594 (800 pg; red) was injected into two dorsal blastomeres of four-cell-stage embryo. For results in Figs. 8A and 8B, dorsal open-faced explants were made at stage 10 (as in A), and then clumps of about 10 cells (for small populations) or hundreds of cells (for large populations) of the mesodermal region were removed from the *Xstbm* + *GFP*-injected (middle row) and *GFP*-injected (bottom row) explants and wedged into Alexa594-injected explants (top row). For results shown in Fig. 9, clumps of about 10 cells (for small populations) and hundreds of cells (for large populations) were removed from the Alexa594-injected explants (top row) and wedged into *Xstbm* + *GFP*-injected explants (middle row). (C) To analyze the effects of *Xstbm* on neural convergent extension for results in Figs. 8C and 8D,

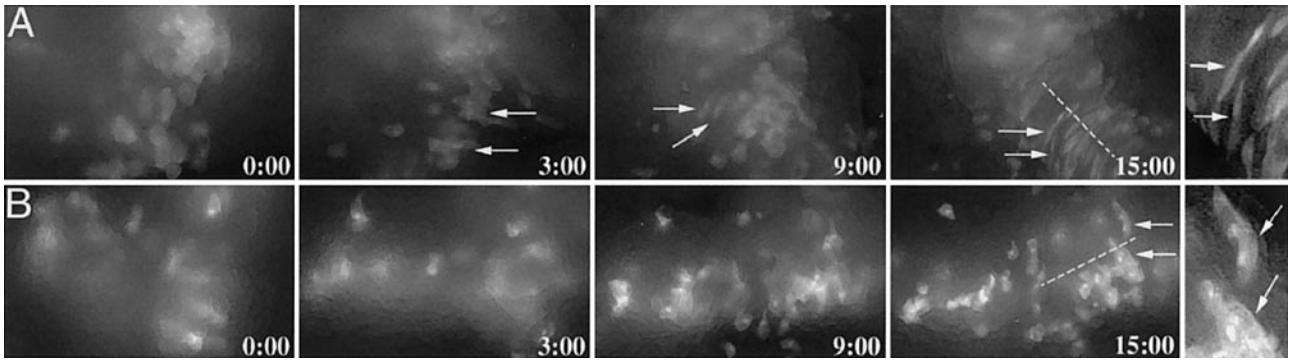

FIG. 7. Frames from time-lapse movies of fluorescently labeled cells show that cells of explants made from normal embryos adopt the bipolar (arrow), mediolaterally oriented protrusive activity typical of this region (notochord) and intercalate between one another during convergence and extension (A), whereas the cells of explants made from *Xstbm*-injected embryos show unorganized protrusive activity and did not form the bipolar cells characteristic of the prospective notochord region (B, arrow). An enlargement of the last frame is shown at the far right. The direction of anterior–posterior axis is indicated by the dashed line, anterior at the bottom. The time elapsed is indicated at right bottom. This figure is presented in a gray-scale version because the contrast is better than it is in the two-color version.

tive neurons, is normally organized in three mediolaterally positioned longitudinal stripes and an anterior, lateral spot (Fig. 5E) (Chitnis *et al.*, 1995). In *Xstbm*-injected embryos, its expression is perhaps somewhat decreased, but the rudiments of at least two and perhaps three stripes, as well as the characteristic anterior lateral spot, are expressed (Figs. 5E and 5F, see numbers). However, due to the failed convergence, these patterns arc around both sides of the open blastopore, rather than lie along the midline where convergence and extension would have brought them (Figs. 5E and 5F). The lesser expression is expected since this characteristic pattern of neural cell differentiation may depend to some extent on mediolateral tissue interactions in the neural plate/tube (Tanabe and Jessell, 1996), which would be disrupted by the absence of convergence along the mediolateral axis. Thus, these results suggest that overexpression of *Xstbm* inhibited neural fold closure without direct effects on neural differentiation.

Mesoderm Extension Is Also Blocked by Xstbm

The mesodermal component of the dorsal tissues of *Xstbm*-injected embryos was also very short and failed to converge and extend. Whole-mount *in situ* hybridization for *chordin*, expressed in the notochord, shows that this structure is very short, wide, and thick, compared with the normal notochord (Figs. 5G–5J). The somitic marker *MyoD* was expressed far laterally, widely separated from midline, around the unclosed blastopore, in its unconverged, unextended position (Figs. 5K and 5L), reminiscent of the position of the somites on the fate map (see Keller, 1991). However, the amount of tissue expressing these markers is comparable to that seen in normal embryos, suggesting that *Xstbm* overexpression inhibited mesodermal extension without effects on its differentiation.

Both Mesodermal and Neural Convergence and Extension Are Inhibited by Xstbm Overexpression in Explants

In the whole embryo, the mesodermal and neural convergence and extension machines act in parallel (see Keller *et al.*, 2000), and inhibition of either neural or mesodermal convergence and extension alone could offer enough resistance to the other, unaffected partner to cause it to fail. Therefore, we tested the effect of overexpression of *Xstbm* in explants in which the mesodermal and neural convergence and extension machines lie in series rather than in parallel. Neither the mesodermal nor the neural components of the dorsal sandwich explants made from the

Xstbm + *GFP* (200 + 200 pg; middle row), *GFP* (200 pg) mRNA (green, bottom row), or Alexa594 (800 pg; red, top row) was injected into two dorsal blastomeres of the four-cell-stage embryo (left column). Dorsal open-faced explants from *Xstbm* + *GFP*- and *GFP*-injected embryos were made at stage 10 as the methods in (A) (second column from left); then clumps of about 10 cells (for small populations) or hundreds of cells (for large populations) of neural region were removed from the *Xstbm* + *GFP*-injected (middle row) and *GFP*-injected (bottom row) explants and wedged into the neural region of Alexa594-injected host embryos (top row) at stage 10 (middle column). After the host embryos developed to stage 12, the dorsal neural and mesodermal tissues were removed and the superficial epithelium peeled off the neural plate at stage 12, exposing the deep cells to time-lapse imaging (two left columns).

Xstbm-injected embryos converged and extended properly (Figs. 5M and 5N). Therefore, the phenotypes of the *Xstbm*-injected embryos are likely to be caused by inhibition of both neural and mesoderm convergent extension.

Overexpression of Xstbm Blocks Normal Polarized Cell Behavior and Cell Intercalation

To determine how *Xstbm* affects convergence and extension, we observed its affects on the polarized cell behavior that normally drives convergence and extension in *Xenopus*, using open-faced explants that allow visualization of cell motility. We used a red fluorescent (Alexa594) dextran and green fluorescent GFP, encoded from injected mRNA, to visualize normal cell behavior, and coinjection of RNA encoding *Xstbm* constructs and *GFP* mRNA to visualize experimentally manipulated cells.

In the first series of experiments, we injected the dorsal region with *GFP* mRNA or with *Xstbm* + *GFP* mRNA at the four-cell stage, thus labeling both controls and experimentals with GFP. We then relabeled several blastomeres with Alexa594 at stage 7, targeting the prospective dorsal mesodermal tissues, thus producing a scattering of Alexa-labeled (red) cells. We then made dorsal open-faced explants at stage 10 (Fig. 6A). In control explants labeled with GFP, the mesodermal cells double-labeled with Alexa594 showed the bipolar, mediolaterally directed protrusive activity characteristic of mediolateral intercalation in the deep mesoderm, and they intercalated with their neighbors very well (white arrows, Fig. 7A). In contrast, in *Xstbm* + *GFP*-injected explants, the mesodermal cells double-labeled with Alexa594 failed to show the characteristic bipolar, mediolaterally oriented protrusive activity and failed to intercalate with their neighbors (Fig. 7B).

Population Size Dependence of the Xstbm Phenotype: Small Populations of Xstbm-Injected Mesodermal Cells Are Rescued by Normal Cells

We grafted *Xstbm*-overexpressing cell populations of different sizes into normal populations of cells to determine whether small populations or individual cells overexpressing *Xstbm* behave differently from large populations. Strips of deep mesodermal cells, without the overlying epithelium, were cut from *GFP*-injected and *Xstbm* + *GFP*-injected dorsal sectors at stage 10 and inserted into a red fluorescent (Alexa594 dextran-labeled) dorsal, open-faced explant, one on each side of the midline at stage 10 (Fig. 6B). The *GFP*-injected control cells (Fig. 8A, green strip on left, white pointer) intercalated smoothly into the Alexa594-injected host cells, but the *Xstbm* + *GFP*-injected cells did not intercalate (Fig. 8A, green strip on right, yellow pointer). However, when the same experiment was repeated using small populations of *GFP* or *Xstbm* + *GFP*-injected cells (Fig. 6B), both the normal cells (Fig. 8B, green clump on left, white pointer) and the *Xstbm* + *GFP*-injected cells (Fig. 8B, green clump on right, yellow pointer) intercalated well between the host cells. Isolated individual *Xstbm* + *GFP* cells, or ones largely surrounded by normal cells, adopted the bipolar, mediolaterally oriented protrusive activity and the mediolaterally elongated shape characteristic of normal convergence and extension by mediolateral cell intercalation (Fig. 8B).

Xstbm Overexpression Also Affects Neural Cell Motility in a Population Size-Dependent Manner

To determine whether neural cell behavior is also disrupted by *Xstbm* overexpression, strips of *GFP*-injected cells and *Xstbm* + *GFP*-injected cells were cut from the dorsal sectors of stage 10 gastrulae and grafted into corresponding positions on each side of the midline of the neural region of Alexa594-injected host embryos at the same stage (Fig. 6C). When the host embryos reached stage 12, deep neural-overmesoderm explants (see Keller *et al.*, 1999; Elul and Keller, 2000) were made from the host embryos. As in the case of the mesodermal cells, the GFP-expressing neural cells (Fig. 8C, green on left, white pointers) intercalated with the red-labeled host cells, whereas the *Xstbm* + *GFP*-injected cells (Fig. 8C, green on right, yellow pointers) failed to do so. However, when we transplanted each small piece of tissue from *GFP*-injected and *Xstbm* + *GFP*-injected embryos into normal host explants (Fig. 6C), both the *GFP* and the *Xstbm* + *GFP*-injected cells intercalated into the host cell populations (Fig. 8D). These results show that *Xstbm*-overexpressing neural cells, like their mesodermal counterparts, can intercalate with normal cells when largely surrounded by normal cells.

Isolated Populations of Normal Cells Show Normal Behavior in a Background of Xstbm-Overexpressing Cells

We have seen that normal cells can provide an environment that will rescue *Xstbm*-overexpressing cells. Conversely, will an environment of *Xstbm*-overexpressing cells inhibit normal cell behavior? To answer this question, large and small pieces of deep mesoderm, without epithelium, were cut from Alexa594-injected dorsal sectors at stage 10 and grafted into corresponding dorsal mesodermal regions of *Xstbm* + *GFP* injected at stage 10 (Fig. 6B). Large patches of normal cells could undergo convergence and extension in the presence of surrounding host *Xstbm* + *GFP*-injected cells, whereas the normal cells in small groups surrounded by host *Xstbm* + *GFP*-injected cells scattered and moved randomly rather than intercalating (Fig. 9, arrow). Moreover, a few *Xstbm*-overexpressing host cells intercalated into the large, normal populations of cells that were grafted into their midst (Fig. 9, pointer). These results show that an island of normal cells in a *Xstbm* host environment can undergo normal cell intercalation behaviors, provided that the populations are large and they can intercalate among themselves. However, normal cells cannot function as individuals in cell intercalation when surrounded by *Xstbm*-overexpressing cells. Again, in these experiments,

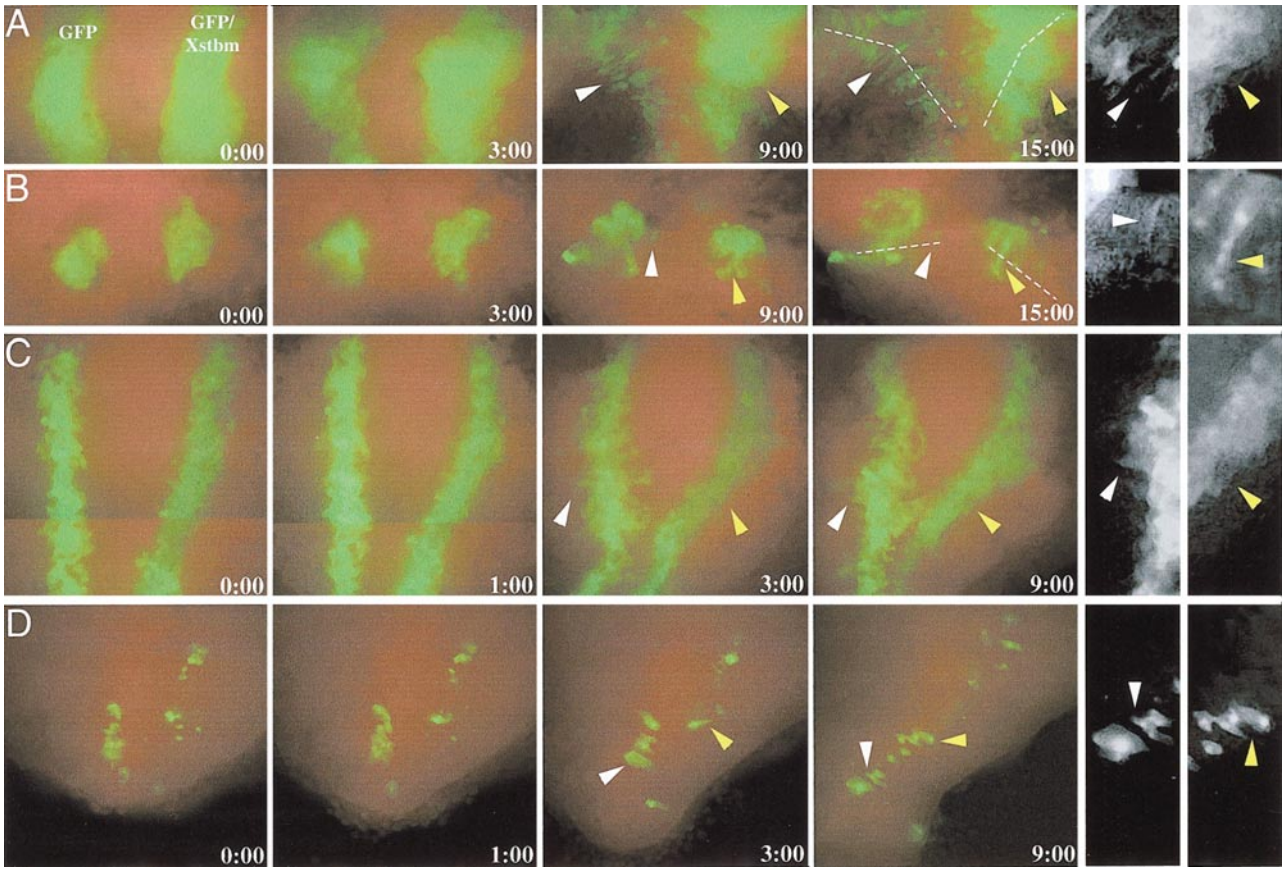

FIG. 8. Time-lapse movie frames show differences between the behavior of normal GFP-injected cells (green-labeled cells on left of each frame) and the behavior of *Xstbm*-injected cells (green-labeled cells on right of each frame) grafted into normal, Alexa594 dextran-labeled host explants (red background) in the dorsal mesodermal (A, B) and neural (C, D) regions. The two far right columns are high magnifications of the last frame of the *GFP*-injected (left) and *Xstbm + GFP*-injected cells (right). The explants were prepared as described in Fig. 6B for mesodermal explants and Fig. 6C for neural explants. A large population of normal cells intercalated into the host explants and form the bipolar cells in the prospective notochord region (green labeled group on left, A). In contrast, a large population of *Xstbm*-injected cells could not intercalate into the mesodermal region of the host explant (green labeled group on right, A). However, small populations of both normal cells (green labeled cells on left, B) and *Xstbm*-injected cells (green labeled cells on right, B) could intercalate among the host explant mesodermal cells. In the neural region, large populations of normal neural cells could intercalate into the normal neural host cells (green labeled group on left, C), whereas *Xstbm*-injected neural cells could not intercalate (green labeled group on right, C). However, small populations of both normal neural cells (green labeled cells on left, D) and *Xstbm + GFP*-injected neural cells (green labeled cells on right, D) could intercalate into the neural region of host explants. The anterior–posterior axes in the mesodermal explants (A, B) are vertical with anterior at the bottom at the outset (0:00) but become tilted in the course of convergence and extension (dashed lines). The anterior–posterior axes in the neural explants (C, D) are vertical with the anterior at the top. The time elapsed is indicated at bottom right.

Xstbm-overexpressing cells at the edge of large, normal cell populations were rescued by the normal cell populations.

Analysis of Functional Domains of Xstbm: The PDZ-Binding Region

Xstbm has a PDZ-binding motif (PDZ-B) at the C terminus, which may interact with PDZ-containing proteins. Supramolecular complexes can be formed by proteins containing PDZ and PDZ-B domains (Saras and Heldin, 1996; Sheng and Sala, 2001). Therefore, we made *Xstbm(ΔPDZ-B)*, which lacks the PDZ-binding region at its C terminus (Fig. 10A). When progressively larger amounts of synthetic *Xstbm(ΔPDZ-B)* were injected into the prospective dorsal marginal zone of the two dorsal blastomeres of the four-cell embryo, a dose-dependent inhibition of convergence and extension occurred (Fig. 10B, 3 left bars) that parallels the effect of increasing amounts of the full-length *Xstbm* (Fig. 4), although about fivefold more of the former was necessary to achieve the equivalent response, assuming the RNAs are similar in stability and efficiency of translation. However, when increasing proportions of *Xstbm(ΔPDZ-B)*,

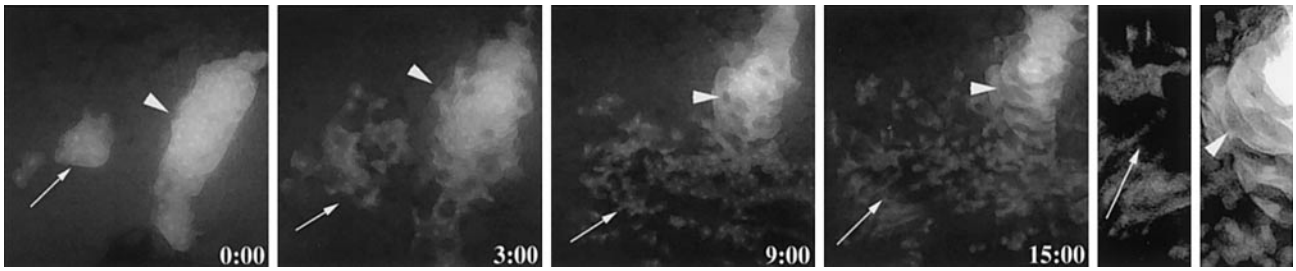

FIG. 9. Frames from time-lapse recording show that a large population of normal cells can intercalate between one another and converge and extend with a surrounding host population of *Xstbm*-injected cells, and that at the border of the two, the *Xstbm*-injected (dark cells) and normal cells (light cells) can also intercalate between one another, such that the *Xstbm*-injected cells (pointer) wind up among the normal cells. At the far right are high magnifications of the last frame of the time-lapse recordings. The *Xstbm*-injected cells adopted the normal bipolar shape within the large population of normal cells (pointer). In contrast, the cells of the small, normal population move and spread out into the *Xstbm*-injected cells, but they did not adopt the bipolar shape, did not undergo an organized cell intercalation, and did not contribute to convergence and extension (arrow). The elapsed time is indicated at bottom right. This figure is presented in a gray-scale version because the contrast is better than it is in the two-color version.

relative to *Xstbm*, were injected, a rescuing effect was observed (Fig. 10B, 3 pairs of bars on right). Therefore, *Xstbm(ΔPDZ-B)* shows a dose-dependent inhibition of convergence and extension, and it offsets the effects of overexpression of *Xstbm* in a dose-dependent manner. These facts suggest that the two act in opposition to one another and that *Xstbm(ΔPDZ-B)* functions in a dominant inhibitory fashion (see Discussion).

Xstbm(ΔPDZ-B) Also Inhibits Cell Movements

To determine whether *Xstbm(ΔPDZ-B)* has the same effects as *Xstbm* on cell behavior, we coinjected *Xstbm(ΔPDZ-B)* and *GFP* into several blastomeres of dorsal marginal zone at stage 7 and then made open-faced explants for visualization of cell behavior. The *Xstbm(ΔPDZ-B)*-injected cells failed to intercalate when introduced as a large, cohesive population (Fig. 11, right), but they intercalated among the uninjected, normal cells when introduced as a dispersed population (Fig. 11, left), similar to the results with *Xstbm*.

Analysis of Functional Domains of Xstbm: The Transmembrane Domains

Xstbm has four putative transmembrane regions, suggesting that it may be inserted into and function in the plasma membrane, or perhaps in the internal membranes of the cell. Therefore, we made *Xstbm(ΔTM)*, a construct that lacks the transmembrane (TM) domains (Fig. 10A). *Xstbm(ΔTM)*-injected embryos showed the same phenotype as *Xstbm* in a dose-dependent manner, although as with *Xstbm(ΔPDZ-B)*, much more (about 8-fold) *Xstbm(ΔTM)* was necessary to produce the severe affected phenotype (Fig. 10C, 3 left bars). However, *Xstbm(ΔTM)* had synergistic effect compared with *Xstbm* alone (Fig. 10C, 3 pairs of bars on the right), rather than the antagonistic effect of *Xstbm(PDZ-B)*. We suggest that *Xstbm(ΔTM)* may have a function similar to *Xstbm* but with reduced effectiveness due to absence of the transmembrane region and membrane localization (see Discussion).

DISCUSSION

Xstbm Is a Xenopus Homolog of strabismus

The predicted amino acid sequence of Xstbm described above, is highly conserved in other vertebrates, such as in the mouse (Ltap; see Kibar *et al.*, 2001) and in humans (KIAA1215; see Nagase *et al.*, 1999), as well as in *Drosophila* (Wolff and Rubin, 1998). The Xstbm described here differs by 6 amino acids from *Xenopus strabismus* described by others (Park and Moon, 2002; Darken *et al.*, 2002) and is probably the same gene, rather than a second one, which is a distinct possibility in this tetraploid species.

Too Much or Too Little Xstbm Inhibits Convergence and Extension

Several observations argue that a proper level of Xstbm activity is required for convergence and extension, with either too much or too little resulting in retardation of these movements. First, the timing and spatial pattern of expression are more consistent with the notion that high levels of *Xstbm* inhibit convergence and extension but lower levels are required for these movements. We and others (Darken *et al.*, 2002) find that *Xstbm* is expressed most strongly in the anterior neural region of *Xenopus*, which does not converge and extend, and the same is true in the zebrafish (Park and Moon, 2002). In contrast, it is expressed at lower levels in the axial (notochordal) mesoderm and throughout the posterior neural plate and neural tube, all regions that converge and extend. Moreover, the levels of mRNA expression rise most strongly (stage 15), some time after convergence and

extension have begun (stage 11) and are, indeed, well underway or have nearly run their course in more anterior regions. Second, overexpression of *Xstbm* inhibits convergent extension in our studies above, as well as those of others (Park and Moon, 2002; Darken *et al.*, 2002). Third, the idea that some level of Strabismus is required for convergence and extension is supported by the fact that morpholino-mediated repression of Strabismus in *Xenopus* (Darken *et al.*, 2002) and in the zebrafish (Park and Moon, 2002), as well as the loss-of-function mutation of *Ltap* in the mouse (Kibar *et al.*, 2001), all result in reduced convergence and extension. Finally, the fact that expression of *Xstbm(ΔPDZ-B)*, which we argue below reduces *Xstbm* function, also retards convergence and extension supports the idea that some level of Strabismus function is necessary for these movements. In summary, our results suggest that either enhancing or reducing the function of Strabismus from some optimal level retards convergence and extension. The negative effect on cell polarity of either an over- or underexpression appears to be a characteristic of a number of components of the planar cell or tissue polarity pathway (see Discussion in Darken *et al.*, 2002).

Xstbm(ΔPDZ-B) Acts Antagonistically to Xstbm, Supporting the Idea That Xstbm Functions in a Complex Mediated by Interaction of the PDZ-Binding Domain with PDZ-Containing Proteins

The PDZ-binding domain suggests that Xstbm participates in PDZ-mediated interactions with other proteins in a complex (Fig. 12). A prime candidate for such an interaction is Dishevelled, the PDZ-domain protein functioning in the planar cell polarity pathway of *Drosophila* (Klingensmith *et al.*, 1994; Krasnow *et al.*, 1995; Axelrod *et al.*, 1998; Boutros and Mlodzik, 1999) and vertebrates (Sokol, 1996; 2000; Wallingford *et al.*, 2000; Tada and Smith, 2000; Heisenberg *et al.*, 2000). Recent evidence shows that Dishevelled functions downstream of Wnt/Frizzled signaling to activate RhoA through Daam1, a formin homology protein, in regulation of *Xenopus* gastrulation (Habas *et al.*, 2001). In addition to its Frizzled interactions, Dishevelled also appears to interact with Strabismus; it colocalizes with Dishevelled and Dishevelled coimmunoprecipitates with Strabismus in human cells (Park and Moon, 2002).

Our results show that the PDZ-binding region of Xstbm functions in regulating convergence and extension. Expression of *Xstbm(ΔPDZ-B)*, which lacks the PDZ-binding region, shows a dose-dependent inhibition of convergence and extension similar to that of the full-length construct (*Xstbm*), a result also obtained by Darken *et al.* (2002). One interpretation of this result is that Xstbm and Xstbm(ΔPDZ-B) act by an identical mechanism of enhancement of the normal function of the molecule, and that the PDZ-binding region is not essential for this function of Strabismus. However, the dose-dependent rescue of the *Xstbm* overexpression phenotype by increasing amounts of *Xstbm(ΔPDZ-B)* argues that this construct acts negatively, as an antagonist that represses Xstbm function, and that its dose-dependent effect when expressed alone is due to a dominant, inhibitory effect on normal Strabismus function. These results are consistent with the results of Park and Moon (2002), showing Strabismus interaction with Dishevelled, and they argue that Xstbm serves as a graded regulator of convergence and extension with an optimum level maximizing polarized cell behavior, and either more or less retarding these movements.

How Does Xstbm Function in Regulating Polarized Cell Behavior?

Our results show that Xstbm regulates convergence and extension by controlling some aspect of the underlying polarized cell behavior in both mesodermal and neural tissues. We postulate that Xstbm dimerizes and functions in a complex, probably at the plasma membrane, although function on internal cell membranes is not ruled out (Fig. 12, left panel). Dimerized Xstbm would interact with downstream PDZ-containing proteins through a mechanism requiring cooperative function of the two PDZ-binding regions of the dimer. This mechanism accounts for the antagonistic behavior of the PDZ-binding domain deletion construct, Xstbm(ΔPDZ-B), which would act in a dominant inhibitory fashion by dimerizing with normal Xstbm while failing in the downstream signaling that requires cooperative function two PDZ-binding regions (Fig. 12, middle panel). Expression of Xstbm (ΔPDZ-B) would depress normal levels of Xstbm function below the optimum for polarized cell behavior, and rescue overexpression of Xstbm by reducing the Xstbm-mediated effect on cell polarity back to an optimal value. The weak synergistic effect of the untethered form lacking transmembrane regions Xstbm(ΔTM) and Xstbm could be accounted for if the truncated form would function with Xstbm but less effectively because of the lack of concentration at the membrane (Fig. 12, right panel). As noted above, Dishevelled may be the PDZ protein interacting with Strabismus (Park and Moon, 2002), although interactions with other as yet unidentified PDZ-containing proteins are not ruled out.

A major issue is how Frizzled-mediated and Strabismus-mediated control of convergence and extension are related. Frizzled 7 (Djiane *et al.*, 2000; Medina *et al.*, 2000), Frizzled 8 (Deardorff *et al.*, 1998), and the Frizzled ligand Wnt 11 (Tada and Smith, 2000; Heisenberg *et al.*, 2000) have roles in vertebrate convergence and extension. Recent work provides evidence for Frizzled-mediated signaling through binding of Daam1 with both Dishevelled and RhoA in regulating *Xenopus* gastrulation (Habas *et al.*, 2001).

In studies of *Drosophila*, Van Gogh/Strabismus is regarded as an antagonist in the Frizzled pathway (see Adler *et al.*, 2000; Adler and Lee, 2001) and the same may be the case in *Xenopus*. As with Strabismus, both increase and decrease of Wnt/Frizzled-mediated signaling appears to retard vertebrate morphogenesis (Deardorff *et al.*, 1998; Djiane *et al.*, 2000; Medina *et al.*, 2000; Tada and Smith, 2000; Heisenberg *et al.*, 2000; Winklbauer *et al.*, 2001; Habas *et al.*, 2001). Whether the two act antagonistically in controlling convergence and extension has not been examined directly.

Xstbm might antagonize the Frizzled-Dishevelled signaling pathway by competing with Frizzled for interaction with Dishevelled (Fig. 12). Alternatively, Frizzled and Strabismus may control different aspects of cell polarity through competing downstream pathways.

It is not known what aspects of the bipolar, mediolaterally oriented protrusive activity of the mesodermal cells (Shih and Keller, 1992a,b), or the monopolar, medially directed protrusive activity of the neural cells (Elul and Keller, 2000) is controlled by Strabismus or Frizzled, and whether the two control separate parameters of protrusive activity (Fig. 12). The bipolar mesodermal cells have large lamellipodia medially and laterally and small filopodial contacts anteriorly and posterior, but the underlying cytoskeletal organization of this difference is unknown. The midline-directed neural cell behavior appears to be dramatically different, but this behavior may depend on the presence of an underlying bipolar behavior shared with the mesoderm, but modified by midline signals (see Elul and Keller, 2000; Keller *et al.*, 2000), thus accounting for the common control of both neural and mesodermal cell intercalation by the PCP pathway observed here with Strabismus and previously by others (Wallingford and Harland, 2001).

Is the role of Strabismus in controlling cell polarity in *Drosophila* conserved in vertebrates? *Strabismus/Van Gogh* is a planar tissue polarity gene that functions in the patterning and morphogenesis of the wing (Taylor *et al.*, 1998: Adler *et al.*, 2000; Adler and Lee, 2001) and eye of *Drosophila* (Wolff and Rubin, 1998). In the wing, it has both a cell-autonomous and a dominant cell-nonautonomous function in controlling the polarity of the hairs on the wing epidermal cells (Taylor *et al.*, 1998; Adler *et al.*, 2000). How the positioning and direction of epidermal hairs is related to the bipolar and monopolar cell intercalation behaviors underlying mesodermal and neural convergence and extension is not known, but the fact that Strabismus can now be added to the growing list of common components controlling these superficially different cell polarities suggests that that they have common underlying mechanisms.

Xstbm and Cell Fate

We found no significant effects of overexpression of *Xstbm* on markers associated with cell fate at levels sufficient to block convergence and extension.

Perturbation of Strabismus Function Results in an Open Neural Plate in Both Frog and Mouse

We find that *Xstbm* is expressed more strongly in the neural region than in the mesoderm of *Xenopus*, which is in agreement with Darken *et al.* (2002), and is consistent with L-tap expression in the mouse (Kibar *et al.*, 2001). Although *Ltap* is one of 17 transcripts lacked in the Loop-tail (Lp) mutant (Mullick *et al.*, 1995; Underhill *et al.*, 1999, 2000; Doudney *et al.*, 2001), the Loop-tail mutant has a shortened anterior–posterior axis and a failure of neural plate closure to form a neural tube (Greene *et al.*, 1998; Kibar *et al.*, 2001). These defects are characteristic of both overexpression and the apparent reduction in the function of *Xstbm* by the putative dominant inhibitory form reported here, as well as the overexpression and morpholino-mediated reduction in function reported by others (Park and Moon, 2002; Darken *et al.*, 2002).

Xstbm Could Be Directly or Indirectly Involved in Neural Fold Fusion

Convergence and extension and cell intercalation are directly involved in the final phases of neural tube closure in *Xenopus* (Davidson and Keller, 1999). Therefore, the effect of *Xstbm* on neural fold fusion in frogs, as well as in the Loop-tail mutant of the mouse homolog, L-tap, could be due to a direct effect on the cell intercalation events involved in neural fold closure. However, it is not clear that cell intercalation is involved in mammalian neural tube closure. Perhaps it is more likely that Strabismus-induced failure of neural tube closure is an indirect effect of the lack of cell intercalation and convergence and extension of the entire neural plate. If convergence and extension are greatly reduced, the absence of convergence will make the neural plate too wide for the neural folds to make contact, and therefore they would not fuse even if they were able. In *Xenopus*, we can resolve this issue by assaying the ability of Strabismus-compromised neural folds to fuse with one another by microsurgically apposing them, independent of the convergence of the neural plate.

Cell Interactions: Rescue of Xstbm Overexpression by Normal Cells

The phenotype resulting from overexpression of *Xstbm* is not absolute and cell-autonomous. Cell intercalation behavior of small groups or individual mesodermal and neural cells overexpressing *Xstbm* is rescued when they are largely or partially surrounded by normal cells. The same is true of *Xstbm(ΔPDZ-B)*-expressing cells, which means that normal cells can also correct for a decrease in *Xstbm* function in other cells, if one accepts our interpretation that this construct results in represents a decrease in *Xstbm* function. This suggests that signals from neighboring normal cells can reset whatever imbalance of polarity signals was mediated by increase or decrease of *Xstbm* function. The fact that this occurs only at the edges of the abnormal cell populations and is more effective on small populations suggests a local signal is involved. In *Drosophila*, patches of cells having loss-of-function of Frizzled or Van Gogh (Strabismus) show domineering, cell-nonautonomous effects on the polarity of nearby, normal cells in the wing that suggests a local signaling mechanism (Adler *et al.*, 2000). Normally, *Drosophila* wing cells have distally pointing hairs. A frizzled clone causes the cells distal to the clone to point proximally, toward the clone, instead of distally, and the Van Gogh/strabismus clone has the opposite effect of causing cells proximal to the clone to point proximally,

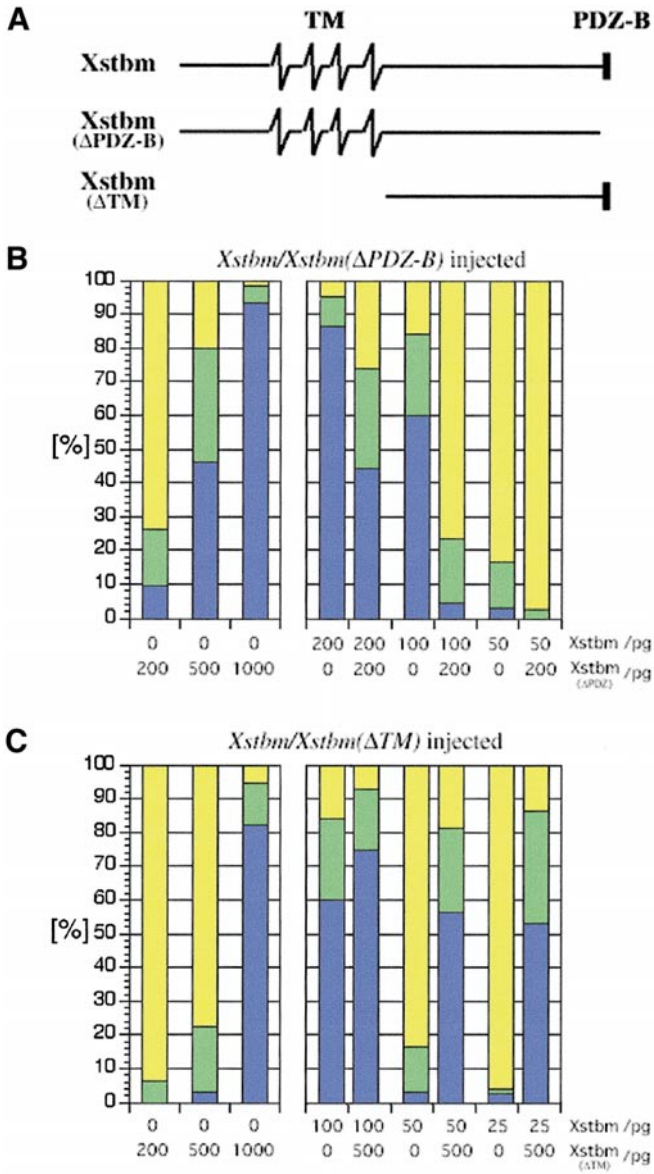

FIG. 10. Diagrams show the structures of the constructs Xstbm, Xstbm(ΔPDZ-B), and Xstbm(ΔTM) (A). The four prospective transmembrane regions (TM) are indicated (107–236) and the black box at the C terminus represents the PDZ-binding motif (518–521) (A, top). Xstbm(ΔPDZ-B), the PDZ-binding domain of Xstbm was deleted (A, middle). Xstbm(ΔTM), the TM domains of *Xstbm* were deleted (A, bottom). Overexpression of increasing amounts of *Xstbm(ΔPDZ-B)* results in a dose-dependent increase in defects of convergence and extension (B, 3 left bars). However, expression of increasing proportions of *Xstbm(ΔPDZ-B)* relative to *Xstbm*, results in a dose-dependent decrease in the severity of the effect of *Xstbm* on gastrulation and convergent extension (B, 3 pairs of bars, right). *Xstbm(ΔTM)* had a synergistic effect when expressed with *Xstbm* (C). *Xstbm(ΔTM)* shows an increasing effect on convergence and extension and gastrulation when expressed alone (C, 3 left bars), and acts synergistically when expressed with *Xstbm* (C, 3 pairs of bars on right). The blue bars represent the proportion of the embryos that showed severely blocked neural fold closure and very short axes as illustrated in Figs. 3E and 3F. The green bars represent the proportion of the embryos that showed impaired neural fold closure as illustrated in Figs. 3C and 3D. The yellow bars represent normal embryos.

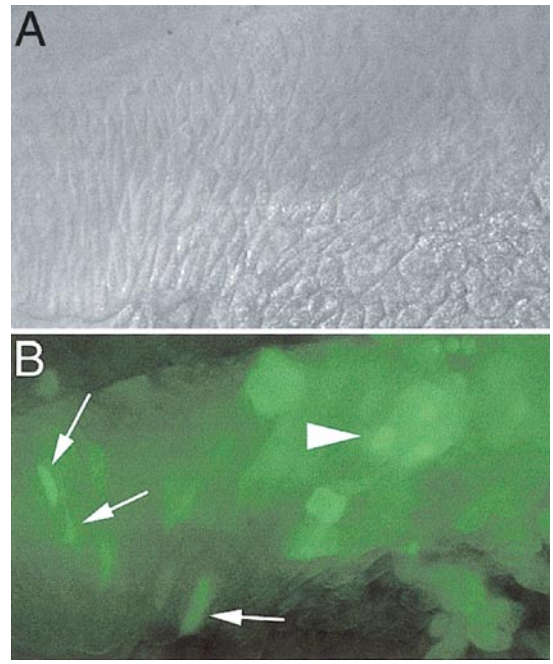

FIG. 11. The effects of *Xstbm(ΔPDZ-B)* on cell polarity. *Xstbm(ΔPDZ-B)* + *GFP* (25 + 5 pg) was injected into several dorsal blastomeres of a stage 7 embryo, and dorsal open-faced explants were made at stage 10. A small, scattered population of *Xstbm(ΔPDZ-B)* + *GFP*-expressing cells was obtained at the left and a large, cohesive population of *Xstbm(ΔPDZ-B)* + *GFP*-expressing cells was obtained at the right of an explant (shown in epi-illumination, A, and in fluorescence, B). Note the elongation and alignment of the cells at the left, whereas those at the right remain rounded (A, B). The scattered, labeled *Xstbm(ΔPDZ-B)*-injected cells intercalated among the unlabeled normal cells (left side) but the cohesive, labeled *Xstbm(ΔPDZ-B)*-injected cells could not intercalate with one another (right side). In this explant, the anterior–posterior axis and axis of extension is left to right.

away from the clone (Adler *et al.*, 2000). Cell ablation experiments suggest that this is due to a local abnormal signal rather than propagation of a long range signal. Patches of *Xstbm*-overexpressing cells in *Xenopus* likewise have no long range effects on cell behavior of surrounding normal cells. In *Xenopus*, we cannot generate patches of complete loss-of-function of the type attainable with *Drosophila* mutants, and thus we do not known if such patches would also have a local cell-nonautonomous affect on normal behavior in this species.

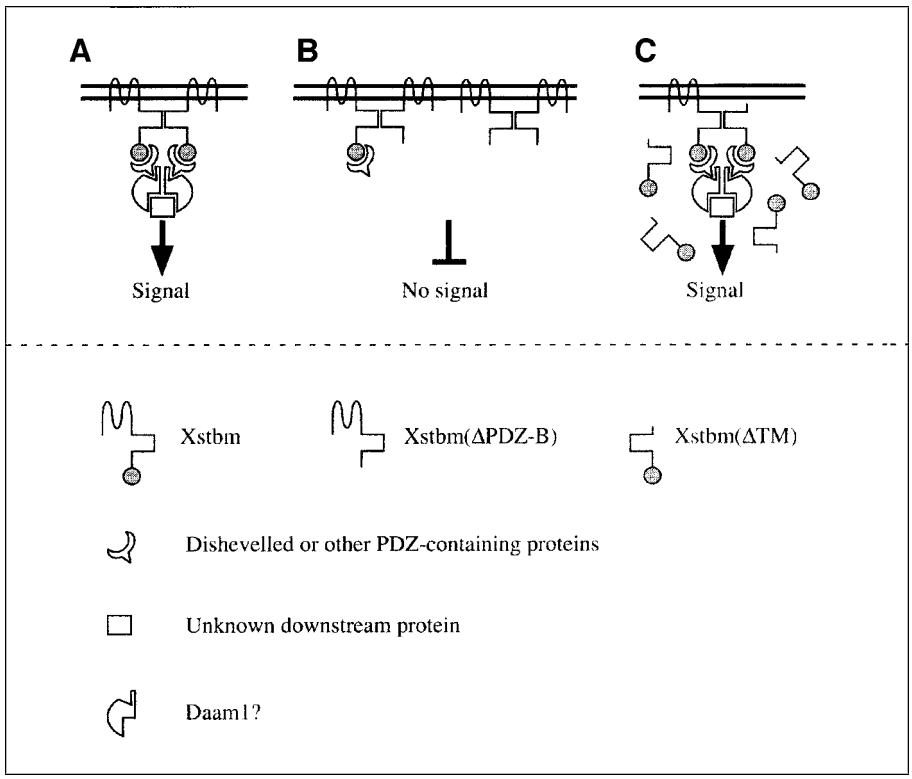

FIG. 12. We propose a model of Xstbm function accounting for our results. Xstbm is localized to the plasma membrane and functions in a complex requiring at least two Xstbm molecules with PDZ-binding domains, that together interact with a PDZ protein or proteins, perhaps Dishevelled (see Park and Moon, 2002), to transduce a signal important in regulating polarized cell behavior (A, left diagram). Overexpression of Xstbm would result in upregulation of this signal and repression of convergence and extension. When Xstbm(ΔPDZ-B), lacking the PDZ-binding region, is expressed, the dimer- or multimer-dependent PDZ-binding function of the complex fails, and no signal or a reduced signal is transduced (B). Increased expression of Xstbm(ΔPDZ-B) would progressively reduce the normal signal level, also leading to failure of convergence and extension. Increased expression of Xstbm(ΔPDZ-B) would also counter the effects of overexpression of Xstbm, resulting in correction of convergence and extension. Expression of Xstbm(ΔTM), lacking the transmembrane regions, would not be localized to the membrane and thus would function inefficiently in increasing the signaling level (C). This would account for the weak additive effect of coexpression of Xstbm(ΔTM) and Xstbm in reducing convergence and extension.

ACKNOWLEDGMENTS

We thank Paul Adler and J. Taylor for helpful discussions on cell polarity, members of the Keller lab, Lance Davidson, and Dave Shook, for their help, and the anonymous reviewers for their constructive comments. This work was supported by NIH Grants HD25594 and HD36426.

REFERENCES

Adler, P. N., Krasnow, R. E., and Liu, J. (1997). Tissue polarity points from cells that have higher Frizzled levels towards cells that have lower Frizzled levels. *Curr. Biol.* **7,** 940–949.

Adler, P. N., and Lee, H. (2001). Frizzled signaling and cell–cell interactions in planar polarity. *Curr. Opin. Cell Biol.* **13,** 635–640.

Adler, P. N., and Taylor, J. (2001). Asymmetric cell division: Plane but not simple. *Curr. Biol.* **11,** R233–R236.

Adler, P. N., Taylor, J., and Charlton, J. (2000). The domineering non-autonomy of *frizzled* and *van Gogh* clones in the *Drosophila* wing is a consequence of a disruption in local signaling. *Mech. Dev.* **96,** 197–207.

Boutros, M., Paricio, N., Strutt, D. I., and Mlodzik, M. (1998). Dishevelled activates JNK and discriminates between JNK pathways in planar polarity and wingless signaling. *Cell* **94,** 109–118.

Axelrod, J. D., Miller, J. R., Shulman, J. M., Moon, R. T., and Perrimon, N. (1998). Differential recruitment of Dishevelled provides signaling specificity in the planar cell polarity and Wingless signaling pathways. *Genes Dev.* **12,** 2610–2622.

Boutros, M., and Mlodzik, M. (1999). Dishevelled: At the crossroads of divergent intracellular signaling pathways. *Mech. Dev.* **83,** 27–37.

Chitnis, A., Henrique, D., Lewis, J., Ish-Horowicz, D., and Kintner, C. (1995). Primary neurogenesis in *Xenopus* embryos regulated by a homologue of the *Drosophila* neurogenic gene Delta. *Nature* **375,** 761–766.

Chomczynski, P., and Sacchi, N. (1987). Single-step method of RNA isolation by acid guanidinium thiocyanate-phenol-chloroform extraction. *Anal. Biochem.* **162,** 156–159.

Darken, R., Scola, A., Rakeman, A., Das, G., Mlodzik, M., and Wilson, P. (2002). The planar polarity gene *strabismus* regulates convergent extension movements in *Xenopus*. *EMBO J.* **21,** 976–985.

Davidson, L. A., and Keller, R. E. (1999). Neural tube closure in *Xenopus laevis* involves medial migration, directed protrusive activity, cell intercalation and convergent extension. *Development* **126,** 4547–4556.

Davidson, L. A., Hoffstrom, B. G., Keller, R., and DeSimone, D. W. (2002). Mesendoderm extension and mantle closure in *Xenopus laevis* gastrulation: Combined roles for integrin alpha(5)beta(1), fibronectin and tissue geometry. *Dev. Biol.* **15,** 109–129.

Deardorff, M. A., Tan, C., Conrad, L. J., and Klein, P. S. (1998). Frizzled-8 is expressed in the Spemann organizer and plays a role in early morphogenesis. *Development* **125,** 2687–2700.

Djiane, A., Riou, J., Umbhauer, M., Boucaut, J., and Shi, D. (2000). Role of frizzled 7 in the regulation of convergent extension movements during gastrulation in *Xenopus laevis*. *Development* **127,** 3091–3100.

Doudney, K., Murdoch, J. N., Paternotte, C., Bentley, L., Gregory, S., Copp, A. J., and Stanier, P. (2001). Comparative physical and transcript maps of approximately 1 Mb around loop-tail, a gene for severe neural tube defects on distal mouse chromosome 1 and human chromosome 1q22–q23. *Genomics* **72,** 180–192.

Elul, T., and Keller, R. (2000). Monopolar protrusive activity: A new morphogenic cell behavior in the neural plate dependent on vertical interactions with the mesoderm in *Xenopus*. *Dev. Biol.* **224,** 3–19.

Greene, N. D., Gerrelli, D., Van Straaten, H. W., and Copp, A. J. (1998). Abnormalities of floor plate, notochord and somite differentiation in the loop-tail (Lp) mouse: A model of severe neural tube defects. *Mech. Dev.* **73,** 59–72.

Habas, R., Kato, Y., and He, X. (2001). Wnt/Frizzled activation of Rho regulates vertebrate gastrulation and requires a novel formin homology protein Daam1. *Cell* **107,** 843–854.

Harland, R. (1991). In situ hybridization: An improved method for *Xenopus* embryos. *Methods Cell Biol.* **36,** 685–695.

Heisenberg, C. P., Tada, M., Rauch, G. J., Saude, L., Concha, M. L., Geisler, R., Stemple, D. L., Smith, J. C., and Wilson, S. W. (2000). Silberblick/Wnt11 mediates convergent extension movements during zebrafish gastrulation. *Nature* **405,** 76–81.

Keller, R. (1991). Early embryonic development of *Xenopus laevis*. *Methods Cell Biol.* **36,** 61–113.

Keller, R. E., and Tibbetts, P. (1989). Mediolateral cell intercalation in the dorsal axial mesoderm of *Xenopus laevis*. *Dev. Biol.* **131,** 539–549.

Keller, R., Poznanski, A., and Elul, T. (1999). Experimental embryological methods for analysis of neural induction in the amphibian. *Methods Mol. Biol.* **97,** 351–392.

Keller, R., Davidson, L., Edlund, A., Elul, T., Ezin, M., Shook, D., and Skoglund, P. (2000). Mechanisms of convergence and extension by cell intercalation. *Philos. Trans. R. Soc. Lond. B Biol. Sci.* **355,** 897–922.

Kibar, Z., Vogan, K. J., Groulx, N., Justice, M. J., Underhill, D. A., and Gros, P. (2001). Ltap, a mammalian homolog of *Drosophila* Strabismus/Van Gogh, is altered in the mouse neural tube mutant Loop-tail. *Nat. Genet.* **28,** 251–255.

Klingensmith, J., Nusse, R., and Perrimon, N. (1994). The *Drosophila* segment polarity gene *dishevelled* encodes a novel protein required for response to the wingless signal. *Genes Dev.* **8,** 118–130.

Krasnow, R. E., Wong, L. L., and Adler, P. N. (1995). Dishevelled is a component of the frizzled signaling pathway in *Drosophila*. *Development* **121,** 4095–4102.

Kuhl, M. K., Sheldahl, L. C., Park, M., Miller, J. R., and Moon, R. T. (2000). The Wnt/Ca^{2+} pathway: A new vertebrate Wnt signaling pathway takes shape. *Trends Genet.* **16,** 279–283.

Kuhl, M., Geis, K., Sheldahl, L. C., Pukrop, T., Moon, R. T., and Wedlich, D. (2001). Antagonistic regulation of convergent extension movements in *Xenopus* by Wnt/beta-catenin and Wnt/Ca^{2+} signaling. *Mech. Dev.* **106,** 61–76.

Marsden, M., and DeSimone, D. W. (2001). Regulation of cell polarity, radial intercalation and epiboly in *Xenopus*: Novel roles for integrin and fibronectin. *Development* **128,** 3635–3647.

McEwen, D. G., and Peifer, M. (2000). Wnt signaling: Moving in a new direction. *Curr. Biol.* **10,** R562–564.

Medina, A., Reintsch, W., and Steinbeisser, H. (2000). *Xenopus* frizzled 7 can act in canonical and non-canonical Wnt signaling pathways: Implications on early patterning and morphogenesis. *Mech. Dev.* **92,** 227–237.

Mlodzik, M. (1999). Planar polarity in the *Drosophila* eye: A multifaceted view of signaling specificity and cross-talk. *EMBO J.* **18,** 6873–6879.

Moon, R. T., Campbell, R. M., Christian, J. L., McGrew, L. L., Shih, J., and Fraser, S. (1993). Xwnt-5A: A maternal wnt that affects morphogenetic movements after overexpression in embryos of *Xenopus laevis*. *Development* **119,** 97–111.

Mullick, A., Trasler, D., and Gros, P. (1995). High-resolution linkage map in the vicinity of the Lp locus. *Genomics* **26,** 479–488.

Nagase, T., Ishikawa, K., Kikuno, R., Hirosawa, M., Nomura, N., and Ohara, O. (1999). Prediction of the coding sequences of unidentified human genes. XV. The complete sequences of 100 new cDNA clones from brain which code for large proteins in vitro. *DNA Res.* **6,** 337–345.

Nieuwkoop, P. D., and Faber, J. (1967). "Normal Table of *Xenopus laevis*." North-Holland, Amsterdam.

Park, W. J., Liu, J., Adler, P. N. (1994). The *frizzled* gene of *Drosophila* encodes a membrane protein with an odd number of transmembrane domains. *Mech. Dev.* **45,** 127–137.

Park, M., and Moon, R. T. (2002). The planar cell-polarity gene stbm regulates cell behaviour and cell fate in vertebrate embryos. *Nat. Cell Biol.* **4,** 20–25.

Rothbacher, U., Laurent, M. N., Dearforff, M. A., Klein, P. S., Cho, K. W., and Fraser, S. E. (2000). Dishevelled phosphorylation, subcellular localization and multimerization regulate its role in early embryogenesis. *EMBO J.* **19,** 1010–1022.

Saras, J., and Heldin, C. H. (1996). PDZ domains bind carboxy-terminal sequences of target proteins. *Trends Biochem. Sci.* **21,** 455–458.

Sater, A. K., Alderton, J. M., and Steinhardt, R. A. (1994). An increase in intracellular pH during neural induction in *Xenopus*. *Development* **120,** 268–280.

Sheng, M., and Sala, C. (2001). PDZ domains and the organization of supramolecular complexes. *Annu. Rev. Neurosci.* **24,** 1–29.

Shih, J., and Keller, R. (1992a). Cell motility driving mediolateral intercalation in explants of *Xenopus laevis*. *Development* **116,** 901–914.

Shih, J., and Keller, R. (1992b). Patterns of cell motility in the organizer and dorsal mesoderm of *Xenopus laevis*. *Development* **116,** 915–930.

Shulman, J. M., Perrimon, N., and Axelrod, J. D. (1998). Frizzled signaling and the developmental control of cell polarity. *Trends Genet.* **14,** 452–458.

Sokol, S. Y. (1996). Analysis of Dishevelled signalling pathways during *Xenopus* development. *Curr. Biol.* **6,** 1456–1467.

Sokol, S. (2000). A role for Wnts in morpho-genesis and tissue polarity. *Nat. Cell Biol.* **2,** E124–E125.

Strutt, D. (2001). Asymmetric localization of Frizzled and the establishment of cell polarity in the *Drosophila* wing. *Mol. Cell* **7,** 367–375.

Strutt, D. I., Weber, U., and Mlodzik, M. (1997). The role of RhoA in tissue polarity and Frizzled signalling. *Nature* **387,** 292–295.

Strutt, H., and Strutt, D. (1999). Polarity determination in the *Drosophila* eye. *Curr. Opin. Genet. Dev.* **9,** 442–446.

Tada, M., and Smith, J. C. (2000). Xwnt11 is a target of *Xenopus* Brachyury: Regulation of gastrulation movements via Dishevelled, but not through the canonical Wnt pathway. *Development* **127,** 2227–2238.

Tanabe, Y., and Jessell, T. M. (1996). Diversity and pattern in the developing spinal cord. *Science* **274,** 1115–1123.

Taylor, J., Abramova, N., Charlton, J., and Adler, P. N. (1998). *Van Gogh*: A new *Drosophila* tissue polarity gene. *Genetics* **150,** 199–210.

Theisen, H., Purcell, J., Bennett, M., Kansagara, D., Syed, A., and Marsh, J. L. (1994). Dishevelled is required during wingless signalling to establish both cell polarity and cell identity. *Development* **120,** 347–360.

Topczewski, J., Sepich, D. S., Myers, D. C., Walker, C., Amores, A., Lele, Z., Hammerschmidt, M., Postlethwait, J., and Solnica-Krezel, L. (2001). The zebrafish glypican knypek controls cell polarity during gastrulation movements of convergent extension. *Dev. Cell* **1,** 251–264.

Underhill, D. A., Mullick, A., Groulx, N., Beatty, B. G., and Gros, P. (1999). Physical delineation of a 700-kb region overlapping the Looptail mutation on mouse chromosome 1. *Genomics* **55,** 185–193.

Underhill, D. A., Vogan, K. J., Kibar, Z., Morrison, J., Rommens, J., and Gros, P. (2000). Transcription mapping and expression analysis of candidate genes in the vicinity of the mouse Loop-tail mutation. *Mamm. Genome* **11,** 633–638.

Vinson, C. R., and Adler, P. N. (1987). Directional non-cell autonomy and the transmission of polarity information by the frizzled gene of *Drosophila*. *Nature* **329,** 549–551.

Vinson, C. R., Conover, S., and Adler, P. N. (1989). A *Drosophila* tissue polarity locus encodes a protein containing seven potential transmembrane domains. *Nature* **338,** 263–264.

Wallingford, J. B., Rowning, B. A., Vogeli, K. M., Rothbacher, U., Fraser, S. E., and Harland, R. M. (2000). Dishevelled controls cell polarity during *Xenopus* gastrulation. *Nature* **405,** 81–85.

Wallingford, J. B., and Harland, R. M. (2001). *Xenopus* Dishevelled signaling regulates both neural and mesodermal convergent extension: Parallel forces elongating the body axis. *Development* **128,** 2581–2592.

Wallingford, J. B., Goto, T., Keller, R., and Harland, R. M. (2002). Cloning and expression of a *Xenopus* orthologue *Drosophila* Prickle. *Mech. Dev.*, in press.

Wilson, P. A., Oster, G., and Keller, R. (1989). Cell rearrangement and segmentation in *Xenopus*: direct observation of cultured explants. *Development* **105,** 155–166.

Wilson, P., and Keller, R. (1991). Cell rearrangement during gastrulation of *Xenopus*: Direct observation of cultured explants. *Development* **112,** 289–300.

Winklbauer, R., Medina, A., Swain, R., and Steinbeisser, H. (2001). Frizzled-7 signalling controls tissue separation during *Xenopus* gastrulation. *Nature* **413,** 856–860.

Wolff, T., and Rubin, G. M. (1998). Strabismus, a novel gene that regulates tissue polarity and cell fate decisions in *Drosophila*. *Development* **125,** 1149–1159.

Wong, L. L., and Adler, P. N. (1993). Tissue polarity genes of *Drosophila* regulate the subcellular location for prehair initiation in pupal wing cells. *J. Cell Biol.* **123,** 209–221.

Zheng, L., Zhang, J., Carthew, R. W. (1995). Frizzled regulates mirror-symmetric pattern formation in the *Drosophila* eye. *Development* **121,** 3045–3055.

Received for publication January 22, 2002
Revised March 25, 2002
Accepted March 26, 2002
Published online May 24, 2002